Developmental Biology **228,** 181–196 (2000)
doi:10.1006/dbio.2000.9940, available online at http://www.idealibrary.com on IDEAL®

Multiple Roles for *four-jointed* in Planar Polarity and Limb Patterning

Martin P. Zeidler,* Norbert Perrimon,*,† and David I. Strutt‡,[1]

**Department of Genetics, Harvard Medical School, 200 Longwood Avenue, Boston, Massachusetts 02115; †Howard Hughes Medical Institute, Chevy Chase, Maryland 20815; and ‡Centre for Developmental Genetics, University of Sheffield, Firth Court, Western Bank, Sheffield S10 2TN, United Kingdom*

Insect cuticles have been a model system for the study of planar polarity for many years and a number of genes required for this process have been identified. These genes organise the polarised arrangement of hairs on the legs, wings, thorax, and abdomen of adult *Drosophila*. It has previously been shown that *four-jointed* is involved in planar polarity decisions in the eye as well as proximal distal leg and wing development. We now present evidence that *four-jointed* is expressed in a gradient through the developing wing and show that it is required for planar polarity determination in both the wing and the abdomen. Clones of cells either lacking or ectopically expressing *four-jointed* cause both autonomous and nonautonomous repolarisation of hairs in these tissues. We propose that the inferred *four-jointed* expression gradient is important for planar polarity establishment and that local inversions of the gradient by the clones are the probable cause of the observed polarity phenotypes. In addition we observe defects in wing vein development. The subtle phenotypes of mutant flies, and the diverse patterning processes in which it is involved, suggest that *four-jointed* may act as a modifier of the activity of multiple other signalling factors.

***Key Words: four-jointed;* planar polarity; abdomen; wing; *Drosophila*.**

INTRODUCTION

The *four-jointed* (*fj*) locus was originally identified as a viable mutation and named on the basis of its phenotype in the distal leg, in which only four of the normal five tarsal joints form. In addition to the tarsal phenotype, mutant individuals display striking reductions in the overall length of the proximal/distal (PD) axis of legs and wings (Brodsky and Steller, 1996; Tokunaga and Gerhart, 1976; Villano and Katz, 1995). The subsequent molecular characterisation of *fj* showed that the gene product encodes a 583-amino-acid type II transmembrane glycoprotein with a predicted signal peptidase cleavage site in the extracellular domain. *In vitro* canine microsomal analysis showed that the C-terminus of the protein is secreted and therefore has the potential to act as a diffusible signalling molecule (Villano and Katz, 1995).

Developmental roles for *fj* have also been investigated by genetic mosaic analysis. This has shown that clones of cells lacking *fj* can act nonautonomously during leg joint development, with wild-type tarsi being fused in the vicinity of mutant tissue (Tokunaga and Gerhart, 1976). More recently we have described a role of *fj* in the developing eye. *fj* is expressed in a gradient through the eye imaginal disc where it acts as part of a redundant "second signal" downstream of the pathways regulated by Unpaired, Wingless, and Notch to polarise ommatidial subunits (Zeidler *et al.*, 1999a). However, no detailed analysis of other roles for *fj* have been described and any potential requirement for *fj* in the establishment of planar polarity in other structures has yet to be determined.

The hairs and scales on insect cuticles have long been a model system for the study of the processes that determine such planar polarity. One mechanism proposed to explain planar polarity determination is that directional information is transmitted across the developing epithelium in the form of a concentration gradient of a polarising molecule (Fig. 1A). This hypothesis was initially based on the analysis of striking nonautonomous repolarisation of epidermal structures following cuticle transplantation experiments in insect systems (Lawrence, 1966; Lawrence *et al.*, 1972; Piefo, 1955). Subsequent studies in the fruit fly *Drosophila melanogaster* have resulted in the identification and characterisation of a number of mutations involved in planar

[1] To whom correspondence should be addressed. Fax: 0114 222 2788. E-mail: d.strutt@sheffield.ac.uk.

0012-1606/00 $35.00

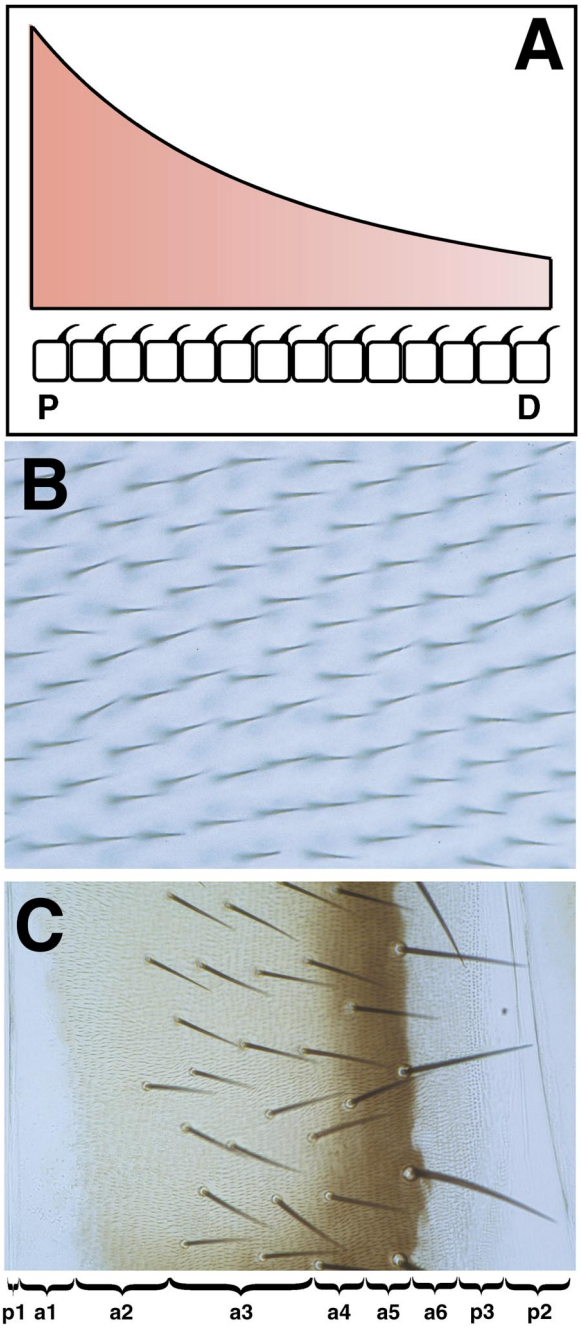

FIG. 1. A model of planar polarity determination in the adult *Drosophila* wing and abdomen. One model (A) suggests that hairs which form at the apical, posterior region of epithelial cells (bottom row) are oriented by the existence of long-range concentration gradients of diffusible polarising molecules (red-shaded graph) which are highest in the proximal (P) and lowest in the distal (D) regions. Such polarising mechanisms orient the hairs present on both surfaces of a wild-type adult wing blade (B) so that they point in a proximal-to-distal direction (only dorsal hairs are shown in this view, distal to the right). Similarly in a wild-type abdominal segment (C) both hairs and bristles are oriented towards the posterior (right). The subdivisions of anterior and posterior compartments in the adult abdomen indicated are as described in Fig. 1A of Lawrence *et al.* (1999a).

polarity establishment (see Shulman *et al.*, 1998, for review).

Although the model described above implies that gradients of molecules may be important at the tissue level, the process of planar polarity determination at the cellular level appears to be controlled by the activity of a signal transduction pathway headed by the seven-pass transmembrane receptor *frizzled* (*fz*) (Vinson *et al.*, 1989). Mutations in *fz* result in disruptions of planar polarity throughout the fly, including randomisation of ommatidia in the eye and swirls of hairs on the wings (Gubb and García-Bellido, 1982; Zheng *et al.*, 1995). Downstream of *fz* in the pathway is the PDZ-containing protein *dishevelled* (*dsh*) (Krasnow *et al.*, 1995), the small GTPase *RhoA* (Strutt *et al.*, 1997), and possibly the Jun N-terminal kinase (JNK) cascade (Boutros *et al.*, 1998). In addition to these components, the seven-pass transmembrane cadherin-type gene *flamingo* is also implicated in the *fz* pathway and has recently been shown to be localised to cell membranes in a *fz*- and *dsh*-dependent manner (Usui *et al.*, 1999). This pathway, possibly acting via cytoskeletal rearrangements induced by RhoA or via gene transcription elicited by JNK/Jun signalling, then establishes the axis of planar polarity within the cell (reviewed in Shulman *et al.*, 1998).

While many of the components of the *fz* signalling pathway have been identified in recent years, the identity of the upstream mechanisms by which the direction of long-range polarity is determined has received less attention. The validity of a gradient-based mechanism for planar polarity determination has, however, been supported by more recent molecular experiments. In these experiments a spatially localised heat shock applied to pupal wings was used to overexpress Fz at the tip of the wing; this treatment is sufficient to reorient wing hairs to point towards the proximal end of the wing and away from the region of ectopic Fz expression (Adler *et al.*, 1997). As overexpression of *fz* has been shown to activate its associated pathway (Krasnow *et al.*, 1995; Strutt *et al.*, 1997) this result is thought to indicate that wing hairs point "down" gradients of *fz* activity. It was therefore suggested that planar polarity in the wild-type wing was the result of an endogenous gradient of *fz* activation and that, given the uniform expression of Fz protein (Park *et al.*, 1994), this is generated by a gradient of *fz* ligand (Adler *et al.*, 1997, and Fig. 1A).

However, while a gradient-based system of long-range planar polarity determination is conceptually appealing, the identification of potential polarising signals has not been straightforward. It has been suggested that the polarising molecule(s) could be a member of the Wnt family (Krasnow *et al.*, 1995), especially given the identification of other Fz-like molecules as Wnt receptors (Bhanot *et al.*, 1996). However, none of the *Drosophila* Wnts tested show any activity in planar polarity determination (Wehrli and Tomlinson, 1998) and none of the other planar polarity mutations appear to encode potential candidates; none are expressed in gradients and none represent potentially diffusible secreted candidate molecules. In part because of

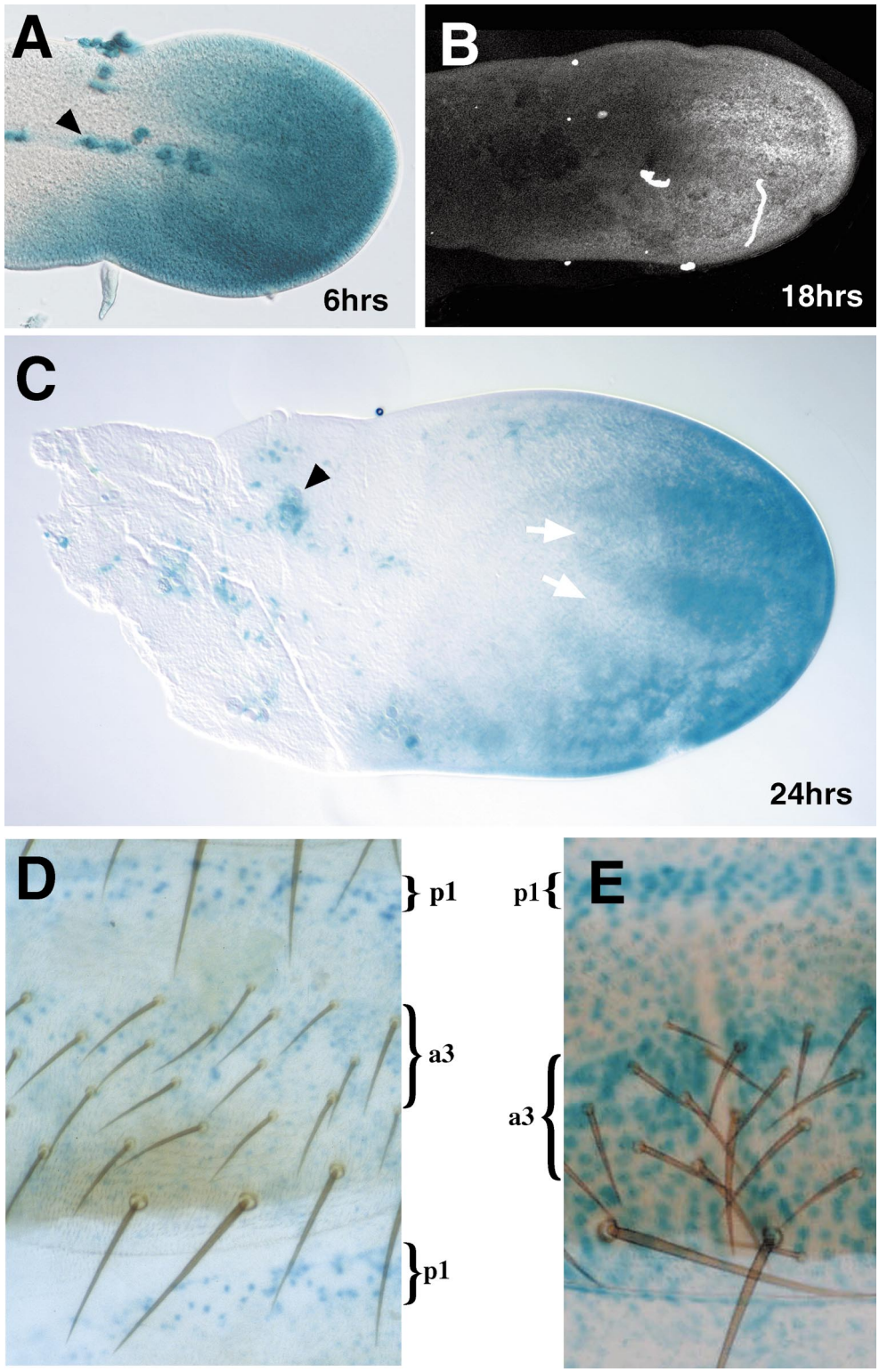

FIG. 2. Expression of *four-jointed* is indicated by the fj^{P1} enhancer detector insertion. In a pupal wing 6 (A), 18 (B), and approximately 24 h (C) after prepupal formation strong staining is detected at the distal end of the wing, which gradually decreases in more proximal regions. Higher levels of staining are also present along the posterior lateral margin of the wing. Lower levels of staining are present in presumptive vein regions (arrows). Distal is right and anterior up. A and C show β-galactosidase activity reactions and B shows an anti-β-galactosidase antibody staining. In young adult abdominal segments (D and E), elevated levels of *fj* staining are detected in two broad bands in the p1 and a3 regions (D). Longer staining of abdomens shows that all regions express some level of *fj* (E). Posterior is down.

this failure to identify gradients *in vivo*, an alternate cell–cell relay-based model of planar polarity determination has also been put forward (Adler *et al.*, 1997; Park *et al.*, 1994). While both models explain many aspects of the phenotypes observed neither have, as yet, gained general acceptance to the exclusion of the other.

Given the role of *fj* in ommatidial polarity determination, we have investigated other tissues in which planar polarity is established (Figs. 1B and 1C) and present further evidence for a role of long-range gradients of *fj* expression in planar polarity determination. Analysis of *fj* enhancer trap expression during development suggests that gradients of *fj* are established in the pupal wing prior to the determination of planar polarity. We show that clones of cells that remove or ectopically express *fj* (and thereby disrupt this gradient) can result in striking planar polarity phenotypes with reversal of wing and abdominal hairs both within mutant tissue and in adjacent wild-type regions. Furthermore we show that although uniform overexpression of *fj* results in only limited disruption of planar polarity, such individuals exhibit shortening of the PD axes of the wings and legs characteristic of the loss-of-function situation. In addition our experiments have also identified previously unrecognised roles for *fj* in anteroposterior growth of the abdominal segments and patterning of the wing veins.

MATERIALS AND METHODS

Histology

Pupal wings were dissected from fj^{P1} individuals and fixed in 1% glutaraldehyde in PBS for X-gal staining (Brand and Perrimon, 1993) or 4% paraformaldehyde in PBS for immunofluorescence using 1:5000 rabbit anti-β-galactosidase (Cappel; see Zeidler *et al.*, 1999b, for further details). Adult abdomens were dissected from newly eclosed adults and fixed in 1% glutaraldehyde for 2–12 h prior to staining. Adult wings were mounted in Euparal (ASCO Laboratories) and abdominal cuticles were mounted in Hoyer's or GMM after a 2- to 3-day incubation in 70% ethanol as described (Struhl *et al.*, 1997b).

Fly Stocks and Genetics

patched-Gal4/UAS-*fj* individuals were raised at 29°C to give the phenotypes shown in Fig. 5D and at 16°C to give the wing shown in Figs. 3B and 6D. *four-jointed* alleles used were fj^{P1} (enhancer detector) and fj^{d1} (null) (Villano and Katz, 1995). Gal4 lines used included *p[actin-Gal4]* (Zeidler *et al.*, 1999a), *p[actin>yellow>Gal4]* (Ito *et al.*, 1997), and *patched*-Gal4 (Speicher *et al.*, 1994). $shavenoid^1$ was recombined onto *FRT42D*, fj^{d1} (Zeidler *et al.*, 1999a) and *FRT42D* (Xu and Rubin, 1993) chromosomes by standard techniques. *y;FRT42D, p[y⁺]* marker chromosome was from the Bloomington Stock Centre. Loss-of-function clones were induced in 24- to 48-h-old larvae by a 1- to 2-h 38°C heat shock while *fj* misexpression clones were induced in 48- to 72-h larvae by a 40-min, 37°C heat shock. The *p[ry⁺, hs-FLP]1* stock (Golic and Lindquist, 1989) was used as a source of FLP recombinase in both cases.

Clonal Analysis

fj^{d1} clonal analysis utilised the *shavenoid* (*sha*) and *yellow* (*y*) markers such that mutant tissue lacked either hairs (*sha*) or pigment (*y*). Only nonautonomous phenotypes of *sha*-marked fj^{d1} clones can be assessed in wing and abdomen due to loss of hairs inside the clone. Regions exhibiting different classes of phenotype are indicated by colours in Fig. 3J. The positions of nonautonomous wing hair inversions induced by loss of *fj* were assessed using 229 *sha*-marked clones present in 88 wings. Of the clones that show nonautonomous phenotypes 6 were present in the orange region and 34 were present posterior to vein 4 in the green and blue regions. Any clone larger than approximately 5 × 5 cells present in the green region gave nonautonomous phenotypes whilst larger clones (typically at least 10 × 10 cells) present in the blue region produced phenotypes. A total of 32 wings containing *yellow*-marked clones (which can be scored only at the wing margin) were scored, with most containing multiple regions of wing hair repolarisations. Inversions were associated with mutant tissue as judged by the rare occasions on which the *y* marker could be scored at the wing margin (Fig. 3E). Polarity phenotypes were observed throughout the grey region (Fig. 3J) and were probably lacking from the most distal regions because the phenotypes only occur on the proximal side of mutant tissue. A composite diagram showing the superimposed phenotypes observed in all 32 wings was generated (Fig. 3C).

Proximal/Distal Phenotype Analysis

Wing regions and abdominal lengths were measured using an eyepiece graticule. For wings each genotype was grown on the same batch of food at the same temperature and mounted within 1–3 days of eclosion after which 15–19 individual wings from different siblings of the same sex were measured. The length of the abdomen between the a1/a2 and a5/a6 boundaries was measured along the midline of abdominal segments 3 to 5. Seventeen segments (from 8 individuals) were counted for wild-type (OreR) and 27 (from 10 individuals) were counted for fj^{P1} homozygous mutants. Average lengths, standard deviation values, and graphical representations were calculated using standard equations and Excel software.

RESULTS

Expression of fj-lacZ

Given the role of *fj* in the establishment of polarity in the *Drosophila* eye (Zeidler *et al.*, 1999a) and the previously proposed significance of expression gradients for the establishment of planar polarity, we investigated *fj* expression in the developing wing using the enhancer detector fj^{P1}, previously shown to accurately mirror the pattern of *fj* mRNA expression *in vivo* (Brodsky and Steller, 1996; Villano and Katz, 1995).

While *fj* expression in the third-instar wing imaginal disc is confined to the wing pouch (Brodsky and Steller, 1996; Villano and Katz, 1995; and not shown) the pattern of expression shown by the enhancer detector at 6 h after prepupal formation (APF) is already graded with lower levels present in proximal regions (Fig. 2A). The graded expression is retained at subsequent stages, as detected both with anti-β-galactosidase antibodies (Fig. 2B) and by *lacZ*

activity staining (Fig. 2C). Note that the large cells seen proximally in Figs. 2A and 2C (arrowheads) are probably macrophages present on the surface of the wing which have endogenous β-galactosidase activity not detected by the antibody used (compare Fig. 2B).

Although there is currently no antibody available against the Fj protein, the previously described fidelity of the *fj-lacZ* reporter suggests that *fj* transcripts (and by implication Fj protein) are present in a gradient in the developing pupal wing, and we refer to this as the *fj* expression pattern.

In contrast to the pattern seen in the wing, the highest levels of *fj* enhancer trap expression present in the abdominal segments of young adults are apparently limited to two transverse bands of small cells located across the a3 and p1 regions of each segment (Fig. 2D). While these bands represent the highest levels of staining at this time, more heavily stained specimens also indicate that a lower level of uniform expression is also present superimposed on the a3/p1 pattern (Fig. 2E). While intriguing, it should be noted that planar polarity has already been established by the time abdomens can be stained and the pattern seen may not mirror *fj* expression present during polarity establishment.

fj and Planar Polarity in the Wing

In light of models which invoke gradients in planar polarity determination and the putative gradient of *fj* expression detected in the developing wing, we examined the wings of *fj* null individuals for defects in planar polarity. While the normal regular pattern of wing hairs pointing towards the distal end of the wing (Fig. 1B) was essentially unchanged in these individuals, occasional minor defects in wing hair polarity were identified (not shown). We therefore carried out a series of misexpression experiments to test for a link between *fj* and planar polarity determination. When *fj* is uniformly expressed using the *actin* promoter and the Gal4/UAS system (Brand and Perrimon, 1993; Zeidler *et al.*, 1999b) occasional examples of wing hair swirls were generated in the proximal regions of the wing (Fig. 3A). Fj was also misexpressed in a stripe along the anterior margin of the anterior/posterior compartment boundary of the developing wing using the *patched*-Gal4 driver line (approximate expression domain shown pink in Fig. 3B). When *fj* is expressed in these cells, nearby wing hairs rotate towards the highest levels of *fj* expression close to the compartment boundary such that they appear to respond to the combined effect of both the endogenous polarising activity in the wing and that generated by the ectopic Fj (Fig. 3B).

Because *fj*-related phenotypes in the eye are associated with clonal boundaries (Zeidler *et al.*, 1999a), and as no suitable clonal markers that did not themselves obscure the polarity of mutant clonal tissue were available, clones lacking *fj* and marked with *yellow* (which can be scored only at the wing margin) were initially generated using the FLP/FRT technique (Xu and Rubin, 1993) and the amorphic fj^{d1} allele. The effect of localised removal of *fj* activity in the wing was found to produce striking disruptions in the normal pattern of wing hair planar polarity (Figs. 3D and 3E) and occasionally result in the loss of wing hairs within the presumptive mutant area (arrowhead in Fig. 3D and not shown). The occasional instances in which the *yellow* marker can be scored (arrows in Fig. 3E) indicate that the phenotypes are associated with fj^{d1} mutant tissue. When plotted together in a composite diagram showing the orientation of disrupted planar polarity associated with clones in many wings ($N = 32$) an overall indication of the potential planar polarity phenotypes that can be induced was obtained (Fig. 3C). This pattern is similar to the phenotype observed in wings from individuals homozygous for hypomorphic *fz* alleles (Adler *et al.*, 1987).

While the unmarked clones indicate that large-scale swirls and hair repolarisation could be induced by *fj* mutant tissue, the cellular autonomy of these phenotypes could not be assessed. We therefore generated loss-of-function mutant fj^{d1} clones in the wing marked by *sha* with which the precise boundary of the clone could be marked and any nonautonomous effects observed. While the sha^{1} allele used has no significant nonautonomous effect (not shown), sha^{1}, fj^{d1} double mutant clones sometimes display striking wing hair planar polarity phenotypes in the wild-type hairs on the proximal side of mutant patches (Figs. 3F, 3G, and 3I). However, clones smaller than approximately 5 × 5 cells never give nonautonomous phenotypes (Fig. 3H).

When the positions of clones that produce nonautonomous phenotypes are plotted we find that only clones present within certain areas generate nonautonomous polarity phenotypes (Fig. 3J and see Materials and Methods). All clones larger than approximately 5 × 5 cells produce nonautonomous phenotypes in a region distal to the posterior cross vein (green in Fig. 3J). Larger clones also produce strong nonautonomous phenotypes in a region between veins 3 and 4 (orange region in Fig. 3J), and weaker phenotypes are observed in a large region in the centre of the wing posterior to vein 4 (blue region in Fig. 3J). We also plotted the positions in which we saw polarity phenotypes induced by unmarked clones and found that this extended throughout almost the entire wing blade (grey region in Fig. 3J), in marked contrast to the limited area in which nonautonomous phenotypes are seen.

While the severity and extent of the phenotypes generated depend on clone position and size, we consistently observe the inversion of wing hair polarity on the proximal side of clones, resulting in the hairs pointing from a region lacking *fj* expression (in the clone) to regions of higher level *fj* expression (in the proximal wild-type tissue). Thus both misexpression and loss-of-function experiments are consistent with wing hairs pointing towards high levels of Fj. It should also be noted that the swirls of hairs associated with the wild-type tissue proximal to sha^{1}, fj^{d1} double clones have a tendency to point towards the posterior of the wing (Fig. 3G). This result appears to be consistent with the composite results obtained from unmarked fj^{d1} single-mutant clones (Fig. 3C) and may be a result of the higher levels of *fj* expressed at the posterior margin of the wing (Figs. 2A–2C).

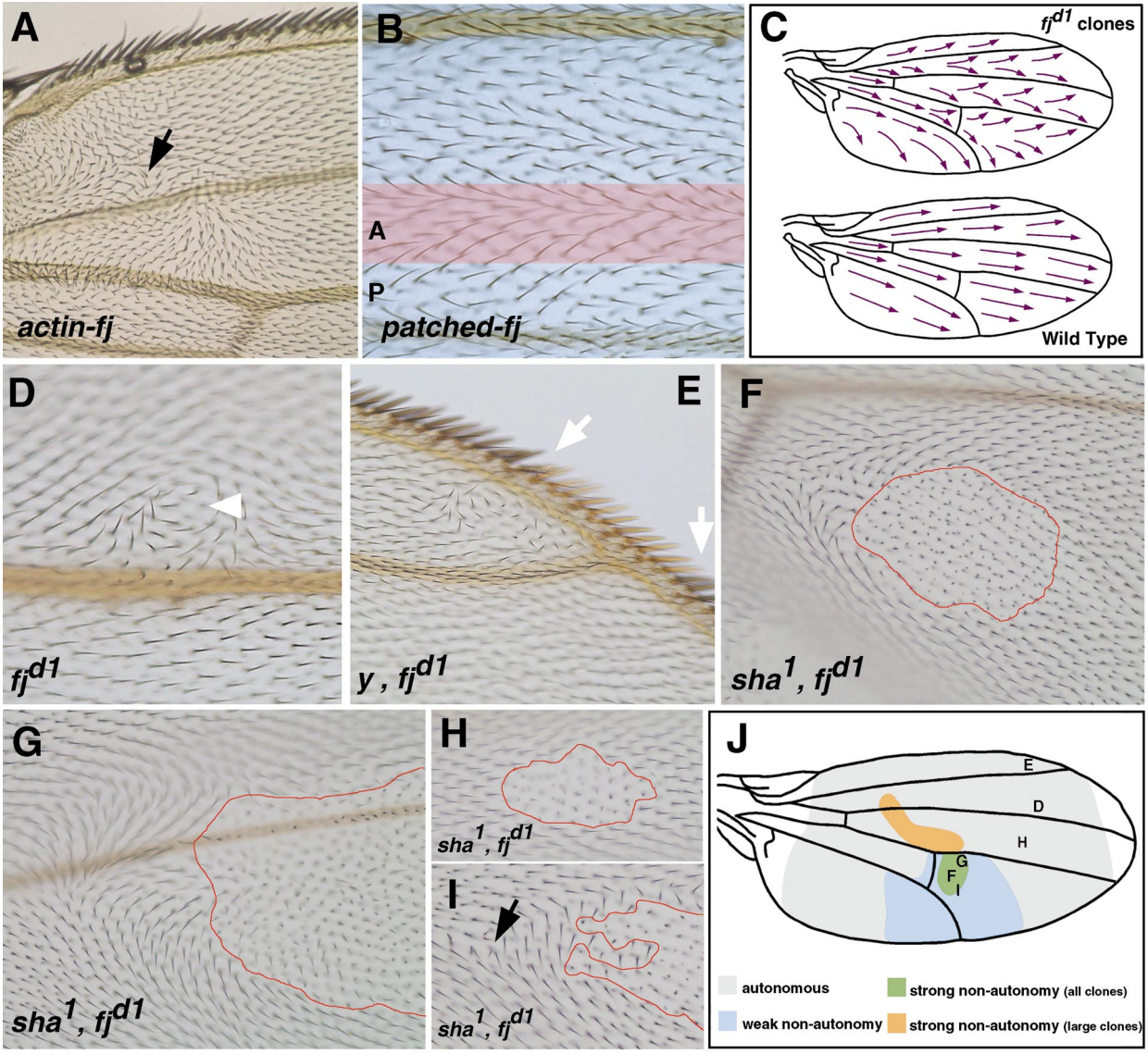

FIG. 3. *four-jointed* causes wing planar polarity phenotypes. Regions lacking *fj* function are marked by the wing hair morphology mutant *shavenoid* and are outlined in red (F to I). All images are labelled according to their genotype and shown anterior up and distal right. (A) Proximal region of a wing uniformly expressing *fj* under the control of *actin-Gal4/UAS-fj*. Wing hair polarity is disrupted, with swirls of hairs forming that include inverted hairs and occasional twinning of wing hairs (arrow). (B) The intervein region between vein 3 and 4 of a wing expressing *fj* under the control of *patched-Gal4/UAS-fj*. Hairs on both sides of the *patched* expression domain (marked in pink) are oriented towards the region of *fj* expression. Anterior (A) and posterior (P) compartments are marked. (C) A composite illustration of the direction of wing hair polarity in multiple wings. In the wild type (bottom) all hairs point towards the distal tip of the wing while in wings containing unmarked fj^{d1} mutant clones hair patterning is disrupted (top). Note the tendency of hairs close to the posterior margin of the wing to point towards this margin. This phenotype is very similar to that produced by weak *fz* mutations (Adler *et al.*, 1987). (D and E) fj^{d1}, *yellow* double mutant clones show autonomous wing hair polarity phenotypes and swirls present in the positions marked in J. While the precise position of the clone cannot be scored the presence of mutant tissue close to the phenotype is confirmed by the *yellow* wing margin bristles present in E (arrows). (F–I) fj^{d1}, sha^{1} double mutant clones in the adult wing blade are outlined in red. The positions of the phenotypes shown are marked in J. Large clones produce nonautonomous inversions on the proximal (left) side of the clone with hairs tending to swirl away and to the posterior of the mutant tissue (F and G). Small clones in general and all clones present in the grey region (J) give no nonautonomous phenotype (H). Occasional twinning of wing hairs (arrow) are also observed associated with double fj^{d1}, sha^{1} mutant clones (I). It should be noted that sha^{1} single-mutant clones also occasionally produce nonautonomous twinning but only in cells immediately adjacent to the clone (data not shown). Taking these results together with the twinning shown in (A) we are confident that this phenotype is a consequence of *fj*. (J) Polarity phenotypes in the adult wing caused by clones of cells lacking *fj*. Autonomous effects (grey) are observed in most areas while strong nonautonomous effects are limited to clones whose posterior margins are present in the green region. Large clones can also produce strong effects in the orange region and weaker phenotypes in the blue region. The positions of the phenotypes shown in D–I are shown by the corresponding small letters in the wing cartoon.

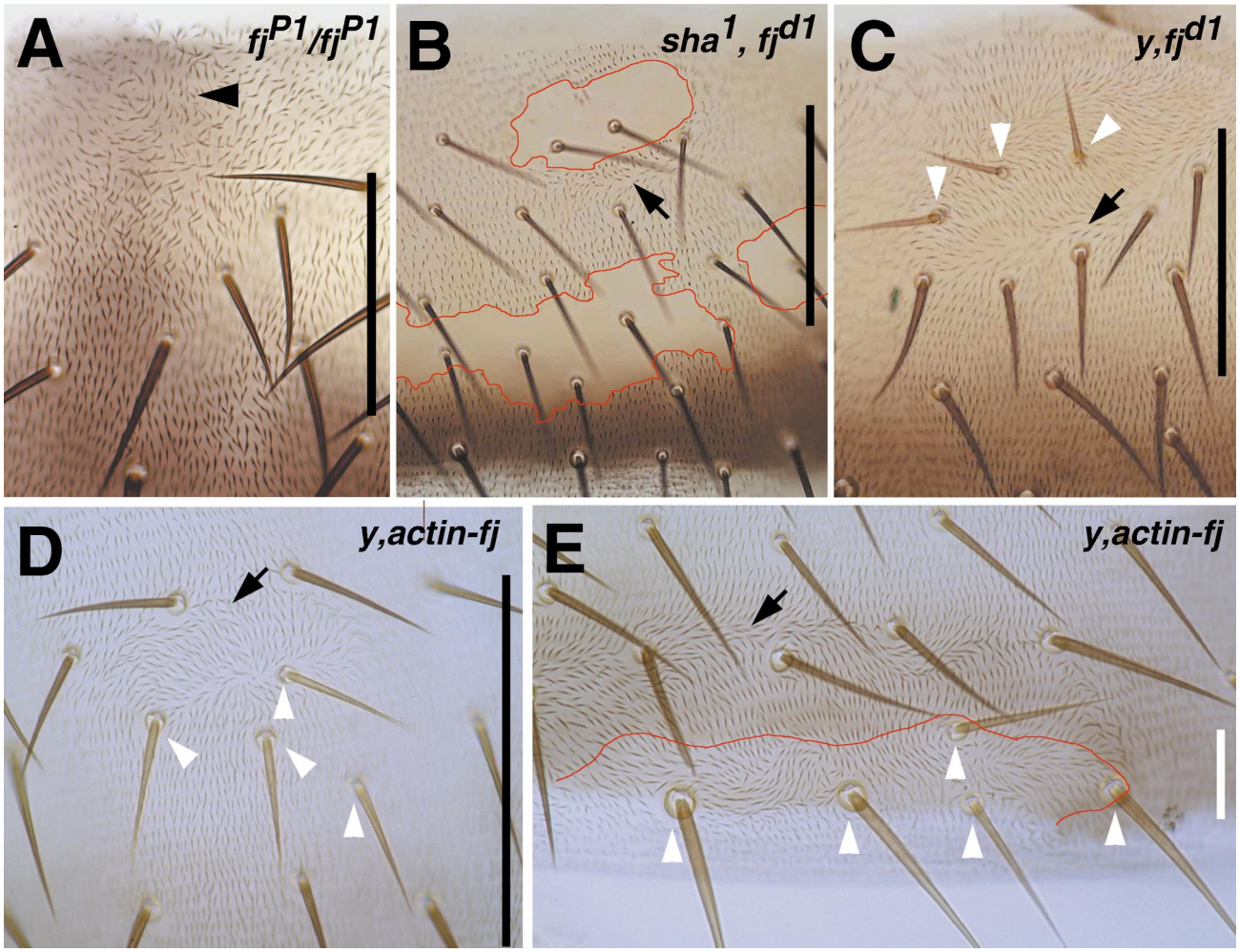

FIG. 4. *four-jointed* and planar polarity determination in the abdomen. All cuticles are shown anterior up and are labelled according to the genotype of the clones shown. Clones in B and E are outlined in red and the a3 region is shown by the black bars in A–D. The white bar in E indicates the extent of the a5 region. White arrowheads indicate *yellow* mutant bristles and black arrows indicate the "parting" where inverted and normally oriented hairs meet. (A) The medial region of a fj^{d1} homozygous mutant abdominal segment showing polarity defects and hair swirls (arrowhead) in the a2 region. Note that more posterior regions (a3–a5) have essentially wild-type polarity. (B) sha^{1}, fj^{d1} double mutant clones marked by the absence of hairs. Clones present in the a5, a4, and posterior a3 regions produce no nonautonomous phenotypes. Clones in a2 and anterior a3 produce approximately three rows of nonautonomous hair inversions at the posterior side of the clone (arrow). (C) A *yellow*, fj^{d1} double mutant clone marked by the loss of pigment in three bristles (white arrowheads) present in the anterior a3 region. Hair inversions are present on the posterior to the clone and extend for approximately eight rows (arrow). (D and E) Clones expressing *actin-Gal4/UAS-fj* marked by the loss of *yellow* pigment in bristles (white arrowheads). In a clone in the anterior a3 region inversions extend for approximately six rows of hairs from the anterior side of the clone (arrow, D). Another *four-jointed*-expressing clone in the a5 region is shown (white bar, E). Because of the higher levels of pigmentation in this region the loss of *yellow* can also be scored in the cuticle itself. Inversions of hairs at the anterior side of the clone extend for approximately seven rows (arrow).

fj and Planar Polarity in the Abdomen

As in the wing, planar polarity in the *Drosophila* abdomen is also exhibited by the polarity of hairs and bristles present on the cuticle of much of each abdominal segment (Fig. 1C). Unlike in the wing, in which only negligible polarity defects were observed, *fj* homozygotes show hair polarity defects in the abdomen, albeit in a very limited region of each segment. In the a2 region of about 50% of fj^{d1} abdominal segments the hairs show extensive "swirls" (arrowhead in Fig. 4A) in a restricted region close to the midline, with weaker phenotypes observed in almost all segments. In addition we also generated two different classes of loss-of-function clones. First we generated sha^{1}, fj^{d1} double mutant clones to identify nonautonomous phenotypes. Interestingly, *fj* does not appear to generate planar polarity phenotypes in the a4, a5, or posterior regions of a3

(Fig. 4B and not shown). Clones positioned in a2 and the anterior of a3 do, however, show clear nonautonomous hair inversions adjacent to the posterior margin of mutant tissue (arrows in Figs. 4B and 7D). While *sha*-marked clones mark the extent of mutant clones, it precludes the analysis of planar polarity within mutant regions. Double-mutant clones lacking the body pigment marker *yellow* and fj^{d1} were therefore induced such that *yellow* mutant bristles in the abdominal cuticle marked the position (but not the precise outline) of the clones. In contrast to the situation in the wing, autonomous phenotypes were found in essentially the same region as the nonautonomous effects described above. Clones in a3–a5 showed no phenotype (not shown), while clones in anterior a3 resulted in major disruptions of hair polarity (Fig. 4C). Given the greater range of inversions apparent in *yellow*- versus *sha*-marked fj^{d1} mutant clones, it is clear that the majority of inverted hairs are present within mutant tissue and that inversions are not restricted to adjacent wild-type cells.

As the loss-of-function clonal analysis indicated that *fj* may be required only in a relatively small portion of the abdomen, we also determined the regions in which *fj* misexpression was sufficient to generate repolarisation using an *actin-Gal4* driver line activated by removal of a $yellow^{+}$ "stuffer" element by FLP recombinase (Ito *et al.*, 1997). In this way *actin-Gal4/UAS-fj*-misexpressing, *yellow*-marked clones could be induced in the abdomen. Clones present in all regions in which the *yellow* marker could be scored (a3–a5) generated polarity inversions at their anterior margins (Fig. 4D). In addition the darker pigmentation present in the a5 region makes it possible to determine the exact outline of the *fj*-misexpressing, *yellow*-marked clone (red outline in Fig. 4E), demonstrating that inversions can extend nonautonomously over at least seven rows of wild-type hairs (black arrow in Fig. 4E).

The results presented regarding hair polarisation in the wing and abdomen are intriguing as it appears that wing hairs point towards high *fj* activity (Figs. 3B and 3G) and that abdominal hairs are oriented away from clones of high *fj* expression (Figs. 4D and 4E). This illustrates that while *fj* can polarise hairs in both abdomen and wing, the direction of polarisation is not invariant and can change from tissue to tissue (see Discussion).

fj and Proximal/Distal Patterning

In addition to the role of *fj* in planar polarity determination demonstrated here, mutations in the locus are associated with both the fusion of tarsal joints and the PD shortening of both leg and wing structures (Brodsky and Steller, 1996; Tokunaga and Gerhart, 1976; Villano and Katz, 1995). During our investigations it became clear that many *fj* misexpression experiments generate PD phenotypes. We therefore compared the phenotypes associated with loss of *fj* to those produced by uniform *fj* misexpression using the *actin-Gal4/UAS-fj* system. In comparison to legs from wild-type flies (Fig. 5A), legs from fj^{d1} homozygotes are clearly shortened and display the characteristic fusion of the second and third tarsi (Fig. 5B). Defects in the legs of *actin-Gal4/UAS-fj* individuals are very similar and include PD axis shortening as well as tarsal fusion (Fig. 5C). While *actin-Gal4*-driven defects were striking, the ectopic *fj* expression driven by the *patched-Gal4* line (Speicher *et al.*, 1994) can produce much more severe phenotypes and can result in extreme PD axis shortening and loss of distal structures while the coxa, a proximal structure, appears largely unaffected (Fig. 5D).

Defects in PD patterning are also evident in the wing. Wild-type wings (Fig. 5E) are longer than those lacking *fj* activity (Fig. 5F) and those in which *fj* is uniformly expressed by the *actin-Gal4/UAS-fj* system (Fig. 5G). In order to better classify the phenotypes obtained, the lengths of different sections of the wing were measured and compared (Fig. 5H). This showed that while proximal regions of the wing are unaffected the region between the anterior and the posterior cross vein is significantly reduced in both the null mutant (fj^{d1}) and the enhancer detector P-element insertion (fj^{P1}) homozygotes as well as in the *actin-Gal4/UAS-fj*-misexpressing individuals (region 3 in Fig. 5H). While the effect on more proximal structures is more variable (region 4 in Fig. 5H) the overall wing lengths are significantly reduced in all cases (total in Fig. 5H). Thus *actin-Gal4/UAS-fj* produces PD defects both qualitatively and quantitatively similar to those produced from the total removal of *fj* in a homozygous amorphic situation.

In addition to the previously characterised role of *fj* in leg outgrowth we also observed that *fj* mutant individuals have shorter and "dumpier" abdominal regions than wild type. In order to quantitate this observation we measured the width of the region of abdominal segments between the a1/a2 and the a5/a6 boundaries. While wild-type abdomens are an average of 261 $\pm$ 12 μm at the dorsal midline, fj^{P1} homozygous abdomens are 221 $\pm$ 12 μm in width (see Materials and Methods). Other *fj* mutants show similar effects (not shown). Thus it is clear that the contraction of PD growth observed in the leg and wing also occurs in the abdomen.

four-jointed and Wing Vein Development

In addition to our observations regarding PD patterning effects, a number of additional observations also indicated a link between *fj* and the patterning of wing veins. Beginning at about 18 h APF we see down-regulation of *fj* enhancer trap expression in longitudinal strips in the wing, which ultimately resolve to a pattern that is thought to represent the future veins (Figs. 2B, 2C, and 6A). In addition to this, wings homozygous mutant for *fj* (Fig. 5F and arrows in Fig. 6B) often contain ectopic wing vein material as do fj^{d1} mutant clones in which vein material forms within or adjacent to the clone (arrow in Fig. 6F and not shown). Furthermore misexpression by *actin-Gal4/UAS-fj* also produces wing vein phenotypes including loss of the posterior cross vein (not shown) and displacement of vein 4 at the junction with the wing margin (Fig. 6C) as well as the deletion of the anterior cross vein in the region of *fj*

misexpression in *patched-Gal4/UAS-fj* wings (Fig. 6D). In some sha^{1}, fj^{d1} double-mutant clones (Figs. 6E–6G) veins are often diverted or duplicated around mutant regions so that the vein material is situated in wild-type tissue immediately abutting the clonal boundary (Figs. 6E and 6F) and in some cases veins "fade" in mutant tissue (Fig. 6G). These results imply that *fj* acts as a regulator of wing vein formation and suggest that in normal development *fj* might function to ensure the precise positioning of the veins.

DISCUSSION

Here we show that *fj* plays a role in the establishment of planar polarity in the wing and abdomen. We have shown that a *fj* reporter, and by implication *fj* itself, is expressed in a gradient through the wing, making *fj* the first identified factor expressed in this pattern that is involved in planar polarity decisions. Additionally we show that clones of cells that either remove or ectopically express *fj* can cause repolarisation of wing and abdominal hairs not only within clones but also in adjacent wild-type tissue and that while loss and misexpression of *fj* have opposite effects in polarity determination, they have very similar effects in PD patterning. Finally we have described an as yet unreported role of *fj* in the development of wing veins.

Molecular Functions of Fj

The molecular nature of Fj and previous results from *in vitro* experimental systems predict that the C-terminus of the Fj protein is potentially secreted (Villano and Katz, 1995). Although this has not yet been unambiguously demonstrated *in vivo*, it is entirely consistent with both the nonautonomous phenotypes that we observe in this study and those previously noted (Tokunaga and Gerhart, 1976; Zeidler *et al.*, 1999a).

The striking differences in phenotype associated with boundaries of *fj* expression compared to uniform loss or overexpression are also noteworthy. This observation appears to be valid for both the *fj*-associated defect in PD patterning and planar polarity. For example, in planar polarity, global loss causes only subtle defects, suggesting that *fj* is largely redundant in this process while loss-of-function clones produce striking repolarisation of wing and abdominal hairs. This behaviour is analogous to phenotypes associated with *fringe* mutations, for which there is only an effect in which boundaries of Fringe-expressing and nonexpressing cells meet (Irvine, 1999; Panin *et al.*, 1997). Fringe is a putatively secreted protein that has recently been shown to act as a glycosyltransferase involved in the modification of the Notch receptor; this modification results in the activation of Notch only at boundaries of Fringe expression (Bruckner *et al.*, 2000; Cho and Choi, 1998; Panin *et al.*, 1997; Yuan *et al.*, 1997). It is interesting to note that in common with *fj*, *fringe* functions both to promote the formation of joints between segments of the leg (Rauskolb and Irvine, 1999) and in establishing polarity in the eye (Cho and Choi, 1998; Papayannopoulos *et al.*, 1998). These parallels between *fringe* and *fj* phenotypes may indicate a similar molecular function, although to confirm this further biochemical and genetic analysis will be required.

Another gene showing parallels with *fj* in polarity determination is *Van Gogh/strabismus* (*Vang*) (Taylor *et al.*, 1998; Wolff and Rubin, 1998). While the precise role of *Vang* in planar polarity determination is as yet unclear, *Vang* produces nonautonomous hair inversion phenotypes on the proximal side of clones and appears similar to *fj* (Taylor *et al.*, 1998). However, the regions of the wing in which *Vang* produces nonautonomous phenotypes are apparently not limited to those in which *fj* acts nonautonomously and further investigations into the potential significance of these observations are required.

Models for Fj Function

While this and previous studies have consistently demonstrated the ability of *fj* to cause nonautonomous effects and influence the establishment of planar polarity (Tokunaga and Gerhart, 1976; Zeidler *et al.*, 1999a) the mechanisms that generate these effects are unclear. In particular, any proposed mechanism must be able to address two key aspects of the *fj* phenotype. First *fj* appears to be largely redundant in polarity determination; while total loss of *fj* does result in rare polarity defects in both the eye and the wing (Zeidler *et al.*, 1999a, and this report) these effects are subtle and the vast majority of hairs and ommatidia lacking *fj* are correctly polarised. This indicates that *fj*-independent mechanisms are largely able to pattern these structures even in the total absence of *fj*. The second key phenotype any model must explain is the inconsistency of *fj* in terms of the direction in which it is able to polarise. As noted in this report, abdominal hairs appear to polarise "down" *fj* gradients while wing hairs polarise "up" (Fig. 7). Similarly in the eye both *fj* and the putative planar polarity receptor molecule *fz* cause nonautonomous polarity inversions on the same (polar) side of clones (Zeidler *et al.*, 1999a; Zheng *et al.*, 1995) while in the wing *fj* and *fz* create nonautonomous polarity phenotypes on opposite sides of clones (Vinson and Adler, 1987, and this report). Thus while both *fz* and *fj* are obviously important for planar polarity determination, and show similar nonautonomous phenotypes (Fig. 3C), *fj* does not function consistently with regard to either itself or other components of the planar polarity determination system.

In an attempt to address these aspects of the *fj* phenotype we have previously proposed that the polarity phenotypes presumed to result from a loss of *fj* were "hidden" because of redundancy with another independent polarising mechanism. This redundancy could, however, be overcome by generating clones that cause a large enough inversion in the direction of *fj* polarising activity to change the overall direction of polarising activity produced by the sum of the two independent systems (Zeidler *et al.*, 1999a). This hypothesis appears to explain both the negligible polarity

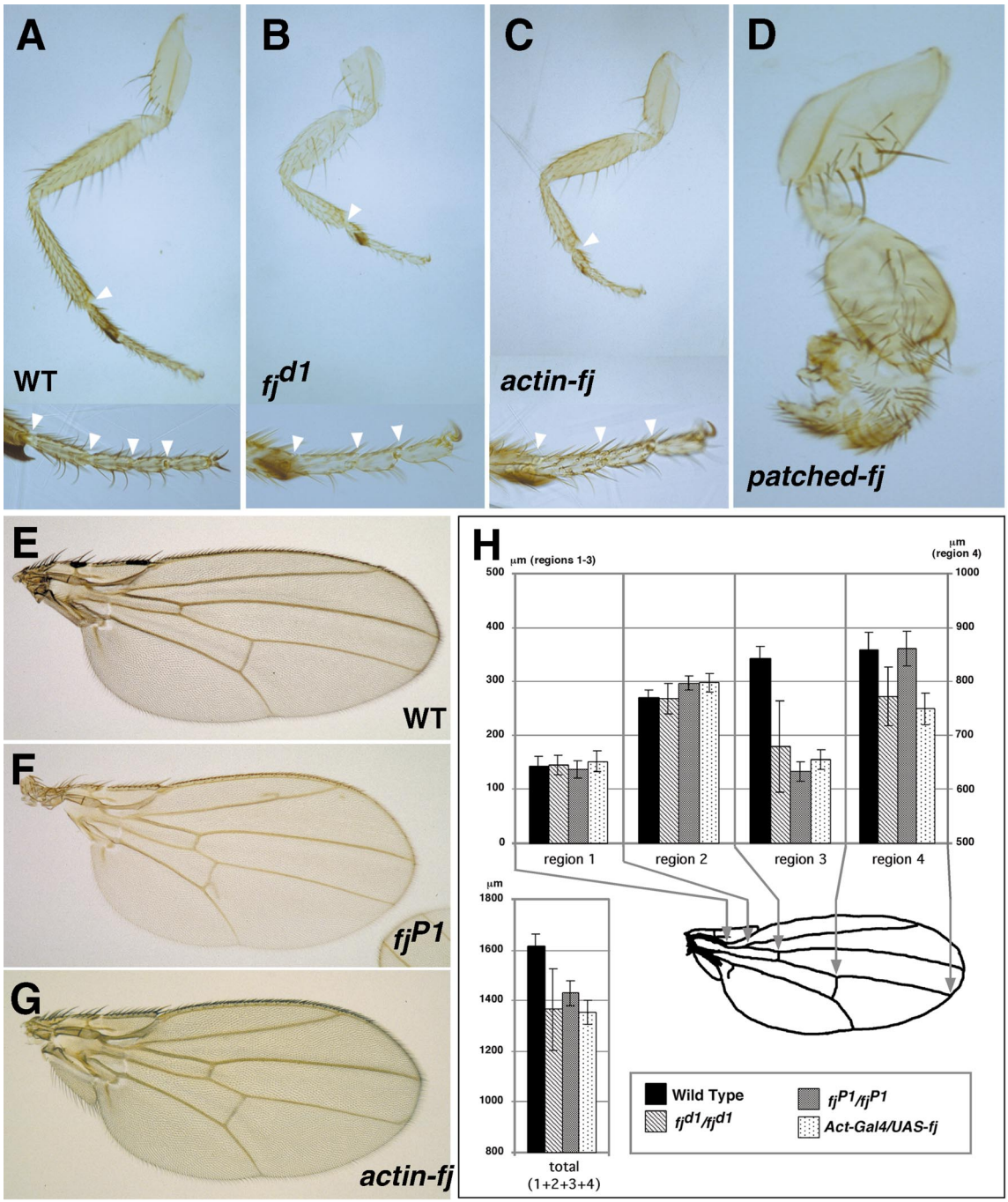

FIG. 5. *four-jointed* and the development of the proximal/distal limb axis. Overviews of whole legs (top) and close-up views of the tarsi (bottom) of the first legs from males that were wild type (WT) (A), homozygous for fj^{d1} (B), or uniformly misexpressing *fj* with an *actin-Gal4/UAS-fj* construct (C). Drastic shortening of the limb along the proximal/distal axis and deletion of a tarsal joint (remaining joints are indicated by white arrowheads) are evident in both loss-of-function (B) and uniform *fj* overexpression (C) backgrounds. Each of (A–D) is shown at the same magnification. Legs dissected from *patched-Gal4/UAS-fj* pharate adults have surprisingly normal coxa but greatly reduced tibia and almost totally deleted tarsal regions (D). Wings of adult females that are WT (E), homozygous for fj^{P1} (F), or uniformly misexpressing *fj* with an *actin-Gal4/UAS-fj* construct (G) are all shown anterior up and at the same magnification. Both loss of *fj* and uniform *fj* overexpression result in a shortening in the overall length of the wing and a reduction in the distance between the anterior and posterior cross veins. Note the patches of ectopic vein material present in the fj^{P1} wing (F). (H) The lengths of four different regions of the wing from the four different genotypes listed in the key were measured. Regions measured are indicated by the overview of a wing, and the average lengths of 15–19 wings are shown in the top graphs. Variation between different wings is expressed as standard deviation error bars. Although results for female wings are shown, shorter male wings show the same qualitative phenotype. The average and standard deviation of the total wing length of each genotype measured are shown on the lower left side. Note that the scale for region 4 is different from that for regions 1, 2, and 3. All measurements are in micrometers.

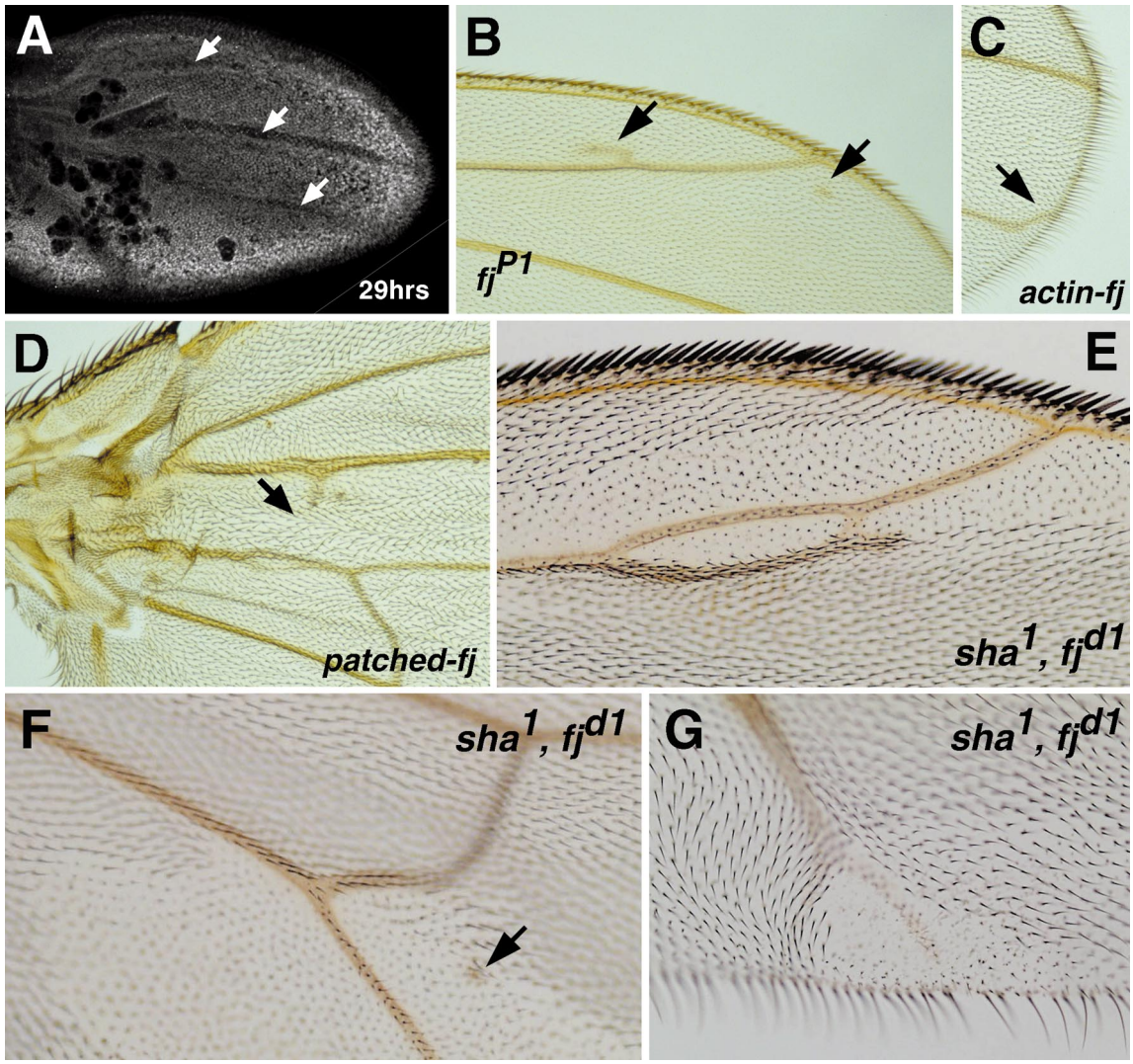

FIG. 6. *four-jointed* plays a role in wing vein patterning. All wings are shown anterior up and distal right. (A) A 29-h APF pupal wing stained with anti-β-galactosidase shows that putative *fj* expression is strongly down-regulated in the presumptive wing vein regions (arrows). (B) fj^{P1} homozygous wings contain ectopic regions of wing vein material (arrows). (C) *actin-Gal4/UAS-fj*-expressing wings frequently show a deviation of vein 4 where it meets the wing margin (arrow). (D) More localised *fj* expression driven by *patched-Gal4/UAS-fj* often deletes the anterior cross vein (arrow) in the region of highest *fj* expression on the anterior side of the compartment boundary. This animal was grown at 16°C. (E–G) sha^1, fj^{d1} double-mutant clones. Some clones contain veins that have been either duplicated (E) or diverted (F) so that they remain in wild-type tissue immediately adjacent to the clone. In addition ectopic regions of wing vein material (arrow in F) are found in many clones and occasional mutant clones are found in which veins fade after entering mutant tissue (G).

phenotypes observed in homozygous *fj* flies and the ability of clones to generate polarity phenotypes.

However, previous results in the eye, considered with the new data presented in this report, also allow for another alternative in which *fj* might be modifying the activity of other polarising pathways or molecules (we will refer to polarising molecules for the sake of simplicity although we have no indication at what point in a polarising pathway *fj* could be acting). In this scenario *fj* activity either reduces or increases the effectiveness of the other polarising molecule and its ability to activate the downstream planar polarity signalling pathway. As the polarising system normally modulated by *fj* is intrinsically capable of determining planar polarity, loss of *fj* results in essentially normal polarity determination. However, clones either lacking or ectopically expressing *fj* generate ectopic boundaries of modified and unmodified polarising molecules such that the resultant changes in activity cause repolarisation of

adjacent hairs or ommatidia. The proposed role of *fj* as a modulator also has an intriguing precedent in vertebrate systems. In the *Xenopus* blastula the secreted molecules Chordin and Noggin are expressed in the Spemann organiser and have been shown to bind to, and inactivate, the BMP-4 ligand. Intriguingly, a gradient of BMP-4-induced pathway activity is present *in vivo* despite uniform levels of ligand expression. This activity gradient is thought to result from the diffusion of the antagonists Chordin and Noggin, which thereby modulate the activity of the underlying signalling system (see Dale and Jones, 1999; Lemaire and Yasuo, 1998, for recent reviews).

While either alternative hypothesis is equally valid given the data available, the second "*fj* as a signal modulator" model is appealing for a number of reasons. First the "signal modulator" model does not require the invocation of a wholly new, as-yet undiscovered, polarising pathway that the "*fj* as a redundant signal" model requires. Second the "modulator" hypothesis allows for the differing directions of repolarisation caused by *fj* in different tissues. In this scenario it is possible that different polarising molecules present in different tissues are each affected by *fj* in different ways. For example, factor X in the abdomen may be negatively regulated by *fj* (see below) while the "second signal" in the eye (Wehrli and Tomlinson, 1998; Zeidler *et al.*, 1999b) would appear to be positively modulated. In both cases uniform loss of *fj* allows the existing polarising activity of factor X (in the abdomen) and the second signal (in the eye) to determine planar polarity and explain the apparent redundancy of *fj* in these tissues.

Planar Polarity Phenotypes of fj

Compared to most other genes affecting planar polarity determination, *fj* is unusual in that it also affects PD patterning in some of the tissues in which it acts, a characteristic which it shares with *dachsous* (Adler *et al.*, 1998). Currently the significance of this is unclear, but it implies that *fj* could affect both processes via a common mechanism. In this context, it is particularly intriguing that *fj* clones give nonautonomous phenotypes only in a region of the wing adjacent to that deleted in *fj* homozygous mutants.

The most straightforward explanation of the polarity phenotypes we observe is by reference to gradient models of planar polarity determination. Given the probable existence of a gradient of *fj* expression in the wing and the putatively diffusible nature of the protein it is possible to explain both the phenotypes and the nonautonomous polarity inversions associated with loss-of-function *fj* clones. In a graphical representation, the predicted Fj gradient in both wild-type wings (Fig. 7A) and wings containing *fj* loss-of-function clones (Fig. 7B) is visualised. If we assume that Fj protein is indeed secreted, the absence of *fj* expression in a loss-of-function clone results in Fj protein from cells outside diffusing into the clone. This diffusion of Fj inverts the Fj activity gradient proximal to the clone (Fig. 7B) such that both wild-type and mutant tissue proximal to the clone are repolarised (red arrow in Fig. 7B). Previous work has suggested that wing hairs point down a gradient of Fz activity and therefore concluded that Fz activity is highest in the proximal regions of the wing (see Introduction and Adler *et al.*, 1997). However, from the work we have presented here it is clear both that *fj* is expressed in a gradient highest at the distal end of the wing and that loss-of-function *fj* clones generate inversions in the gradient of Fj and hair repolarisation at their proximal sides (Fig. 7B). Thus it appears that Fz and Fj act in opposite directions in the wing (as is also implied by the difference in nonautonomy discussed above). A simple model for the phenotypes observed would be that Fj activity ultimately results in a decrease in Fz pathway activity in the wing (blue line in Figs. 7A and 7B).

As *fj* clones throughout almost the entire wing show alterations in which the most proximal hairs of a swirl are inverted in polarity, we infer the presence of a functional gradient of *fj* expression throughout the wing. The observation that strong nonautonomous phenotypes are observed only in a more limited region of the wing can be accommodated if the *fj* gradient is steepest in this region of the wing and thus clones have the strongest effect on the gradient in this area.

The process of pattern formation and planar polarity determination in the adult abdomen has been shown to be dependent on the signalling molecule Hedgehog. In addition to being required in cell fate determination it has been proposed that Hedgehog signalling controls planar polarity indirectly by regulating the expression of an as-yet unidentified factor X (Lawrence *et al.*, 1999a; Struhl *et al.*, 1997a). It is proposed that factor X is expressed in a gradient that is highest at the AP compartment boundary (black line in Fig. 7C and Lawrence *et al.*, 1999a) and causes cells of the anterior compartment to make hairs that are oriented up the factor X gradient (>> symbols in Fig. 7C). Our observations regarding polarity phenotypes in both the anterior regions of *fj* mutant abdomens and the loss-of-function clonal analysis reveal a function for *fj* in a2 and the anterior of a3. However, the lack of *fj* loss-of-function phenotypes in posterior regions rules out the possibility that *fj* might be factor X.

It is, however, clear that *fj* does play some role in polarity determination in a2/anterior a3 regions and that *fj* misexpression is sufficient to alter polarity throughout the regions we can address experimentally (a2 to a6). In this situation the "redundancy" model of *fj* activity discussed above is less compelling and it is easier to think of Fj as a modifier of a signal (factor X) that extends over the entire segment. In this "*fj* as a modifier" model the putative factor X gradient (black lines in Figs. 7D–7F) is modified by the removal (Fig. 7D) or ectopic expression of *fj* (Figs. 7E and 7F) to produce both autonomous and nonautonomous phenotypes similar to those described for the wing above. As clones lacking *fj* have phenotypes only in a2 and anterior a3 regions it is likely that a *fj* gradient is present in these regions and is present at levels too low to produce phenotypes in more posterior parts of the segment (yellow region

in Fig. 7C). However, clones ectopically expressing *fj* are able to modify the factor X gradient at any point (Figs. 7E and 7F). As the gradient of factor X is predicted to be highest at the AP compartment boundary, our experimental observations indicate that *fj* must act as a negative regulator of factor X (see Figs. 7C–7F). This inferred pattern of *fj* expression suggests that *fj* may be acting to steepen the gradient of available factor X present in regions which would otherwise contain only shallow gradients of polarising activity (i.e., farthest from the source of factor X expression at the AP compartment boundary).

The interpretation of our results according to a gradient model of polarity generation does not necessarily imply that *fj* function acts directly to modify *fz* activity. Indeed, the role of *fj* in PD patterning may indicate that a gradient of *fj* is involved in the establishment of "positional values" in the developing wing. In this scenario it is possible that mutant clones misinterpret positional cues such that they assume a more proximal fate than is appropriate given their actual position. In such a case a local repolarisation of wing hairs could then be explained by the action of a short-range polarising system, rather than a long-range gradient over the whole wing. While appealing, this explanation does not adequately explain the planar polarity phenotypes caused by *fj* in either the eye or the abdomen. There is little evidence for patterning defects in *fj* mutant eyes, consistent with alterations in positional values. Furthermore, the positional identity of clones in the abdomen can be scored on the basis of their pigmentation and clones that change this identity have been described to cause rounding of the clone and "sorting out" of the mutant tissue (Lawrence *et al.*, 1999b). Neither pigmentation nor the shape of *fj* mutant clones is affected in a manner consistent with this explanation. While not absolutely conclusive we feel that the gradient model described is more likely to represent the true *in vivo* situation.

Gradients of fj Expression

Given the significance of the *fj* expression gradient little is known about how this pattern is established. In the eye Wingless, Notch, Unpaired, and Fj itself interact to generate a gradient highest at the equator and lowest at the poles (Zeidler *et al.*, 1999a). However, the mechanisms which establish the gradient of *fj* expression in the wing are unknown. The regulation of *fj* by Upd and Wingless signalling does not occur in wing imaginal discs as assayed by misexpression experiments and is not expected given the lack of planar polarity phenotypes associated with Upd and Wg pathway mutants (Axelrod *et al.*, 1998, D.S. and M.Z., unpublished). Furthermore, even the autoregulatory aspect of *fj* expression that occurs in the eye does not appear to be a factor in establishing the gradient of *fj* expression in the pupal wing (not shown).

Other Functions of fj

While this analysis has concentrated on planar polarity a number of observations have indicated a previously unidentified role for *fj* in wing vein formation. It is noteworthy that the expression of *fj* in the developing wing is also significantly weaker in regions thought to represent the presumptive vein regions (Fig. 2A). However, while *fj* appears to have some influence on vein formation it is clear that it does not represent an instructive mechanism as the veins in many clones and mutant wings are often unaffected. Therefore we suggest that *fj* is probably more likely to act to refine the position of veins previously determined by other mechanisms.

Another previously unidentified and unexpected aspect of *fj* activity during development is the striking similarity of *fj* misexpression phenotypes to those associated with loss of *fj* (Fig. 5). One interpretation is that Fj overexpression produced by the Gal4/UAS system may be acting as a dominant negative. While we do not currently have an alternative explanation, we do not think this dominant negative explanation is likely for three reasons. First, the directions of hair repolarisation generated by misexpression and loss-of-function *fj* clones in both the wing and the abdomen are opposite to one another. Second, loss of *fj* generally results in ectopic wing vein material (Figs. 6A and 6D–6F) while its ectopic expression can result in vein loss (Fig. 6C) and third, the phenotypes produced by *patched-Gal4/UAS-fj*-driven overexpression in the leg (Fig. 5D) and wing (Fig. 6D) are far more severe than the phenotypes associated with the total removal of *fj* from the fly. These results indicate that under some circumstances, *fj* misexpression is capable of generating phenotypes opposite to those of loss of function rather than identical to loss of function.

CONCLUDING REMARKS

Here we have shown that *fj* is involved in planar polarity determination in the developing wing and abdomen of the fly. Analysis of an enhancer trap in *fj* suggests that it is expressed in a long-range gradient through the developing wing. We demonstrate that disruption of *fj* expression either by ectopic expression or in loss-of-function clones is sufficient to repolarise the hairs of the wing both autonomously and nonautonomously. Interestingly, *fj* clones exhibit the strongest nonautonomous polarity phenotypes in a central region of the wing that broadly corresponds to the region that is reduced in size in *fj* homozygotes. We have also shown that *fj* plays a role in planar polarity determination in the abdomen where it may act by modifying or acting in concert with an as-yet unidentified polarity signal ("factor X").

Considering these data in conjunction with previously published analysis of *fj* in the eye we propose a model for planar polarity determination in which *fj* is most likely to act to refine or reinforce existing signalling gradients involved in polarity determination.

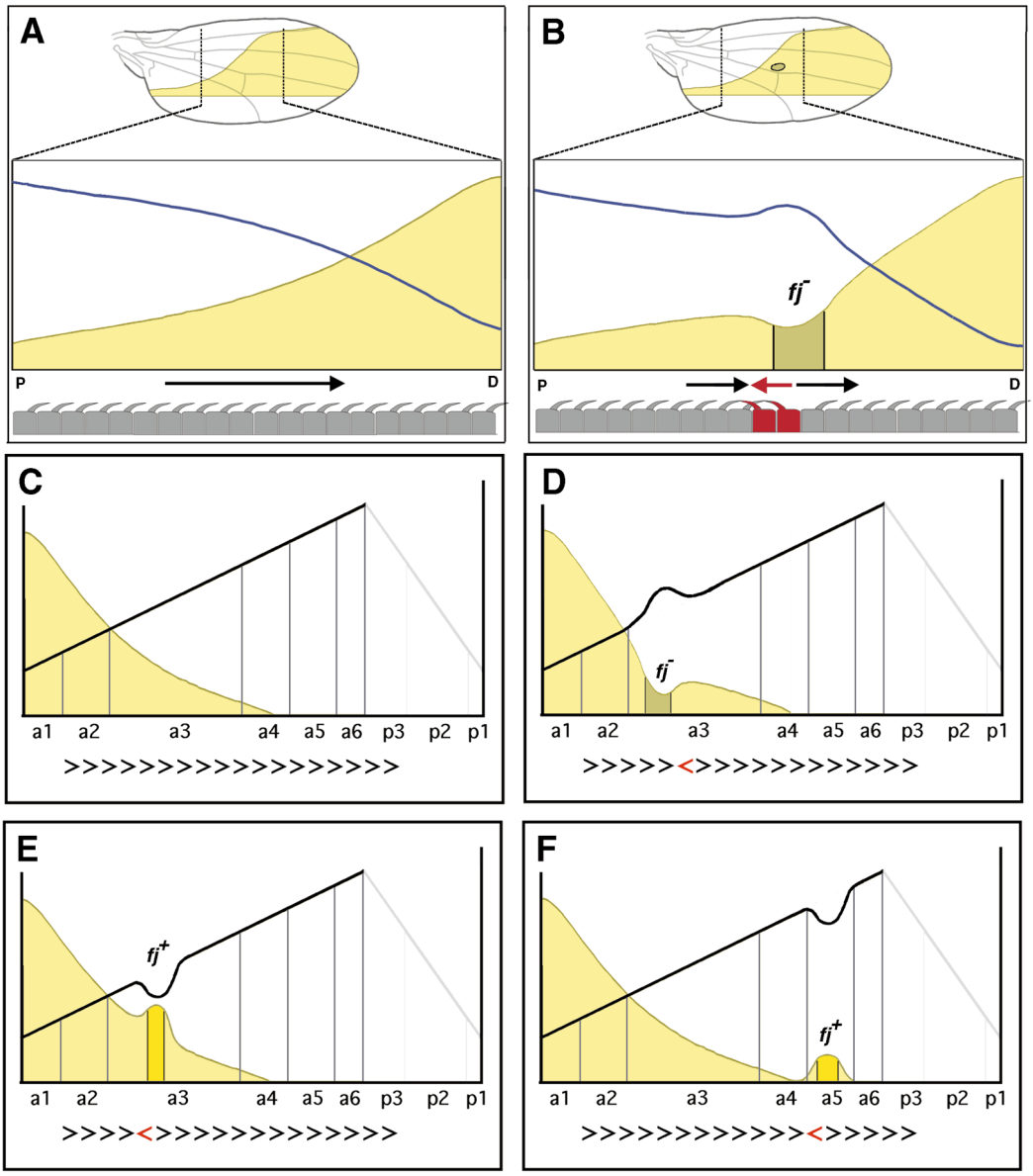

FIG. 7. Diagrams illustrating the slope of polarising activity thought to be responsible for determining planar polarity in the wing (A and B) and the abdomen (C to E). (A and B) The inferred gradient of *fj* observed in the wing is represented by the yellow region and is higher at the distal end of the wing (D) than at the proximal end (P). Cells and the hairs they produce are illustrated in grey. In the wild-type situation (A) hairs are normally oriented and point towards the distal end of the wing (arrow). The gradient of *frizzled* activity thought to be present in a wild-type wing (Adler *et al.*, 1997) is illustrated by the blue line. In a wing containing a clone (grey) lacking *fj* expression (B) Fj protein from surrounding wild-type tissue diffuses into the clone and results in an inversion in the normal Fj activity gradient (red arrow). Both wild-type and *fj* mutant cells are present in this region of inverted gradient and assume an inverted polarity (red cells). The altered gradient of *fz* activity that may ultimately be produced by such a clone is shown as a blue line. Note that based on the *fj* enhancer trap staining pattern, and the stronger clonal phenotypes observed in the middle of the wing, we infer that the *fj* expression gradient is steeper in the central region of the wing (top, A and B). (C to F) The gradient of polarising activity thought to exist in the adult abdomen is highest at the AP compartment boundary that forms between a6 and p3. It is thought that the polarising molecule termed factor X is highest in a6 and lowest in the a1 region (black line) although it is not known what the situation is in the posterior compartment (grey). The inferred pattern of *fj* expression in the segment is indicated by the yellow-shaded region. While no clonal results are available for the a1 region we propose that the gradient present in a2/a3 may be generated at the PA compartment boundary and therefore show it extending through a1 (C). The polarisation of the hairs in the abdominal segment are represented by the direction of the >>> symbols at the bottom of the diagram. In an abdomen containing a *fj* loss-of-function clone (D) the region lacking *fj* (labelled fj^- and shown in grey) actually results in an increase in overall polarising activity, inversion of the polarising gradient (black line) on the posterior side of the clone, and the repolarisation of hairs (indicated by red << symbols) on that side. In abdomens containing clones of cells misexpressing *fj* in either the a3 region (E) or the a5 region (F) the clone (labelled fj^+ and shown as brighter yellow) results in a reduction in factor X polarising activity (black line), inversion on the anterior side, and repolarisation of the hairs on the anterior side of the clone. In both cases the diffusible nature of *fj* results in both autonomous and nonautonomous phenotypes.

ACKNOWLEDGMENTS

We thank Helen Strutt and Michael Boutros for helpful discussions and comments on the manuscript as well as the Bloomington Stock Centre for fly stocks. M.Z. is a Special Fellow of the Leukemia and Lymphoma Society, N.P. is a Howard Hughes Investigator, and D.S. is a Lister–Jenner Research Fellow with additional support from the Wellcome Trust and the MRC. We thank Yorkshire Cancer Research for the provision of a confocal microscope.

REFERENCES

Adler, P., Charlton, J., and Liu, J. (1998). Mutations in the cadherin superfamily member gene *dachsous* cause a tissue polarity phenotype by altering *frizzled* signaling. *Development* **125,** 959–968.

Adler, P. N., Charlton, J., and Vinson, C. R. (1987). Allelic variation at the *frizzled* locus of *Drosophila*. *Dev. Genet.* **8,** 99–119.

Adler, P. N., Krasnow, R. E., and Liu, J. (1997). Tissue polarity points from cells that have higher Frizzled levels towards cells that have lower Frizzled levels. *Curr. Biol.* **7,** 940–949.

Axelrod, J. D., Miller, J. R., Shulman, J. M., Moon, R. T., and Perrimon, N. (1998). Differential recruitment of Dishevelled provides signaling specificity in the planar cell polarity and Wingless signaling pathways. *Genes Dev.* **12,** 2610–2622.

Bhanot, P., Brink, M., Samos, C. H., Hsieh, J.-C., Wang, Y., Macke, J. P., Andrew, D., Nathans, J., and Nusse, R. (1996). A new member of the *frizzled* family from *Drosophila* functions as a Wingless receptor. *Nature* **382,** 225–230.

Boutros, M., Paricio, N., Strutt, D. I., and Mlodzik, M. (1998). Dishevelled activates JNK and discriminates between JNK pathways in planar polarity and *wingless* signaling. *Cell* **94,** 109–118.

Brand, A. H., and Perrimon, N. (1993). Targeted gene expression as a means of altering cell fates and generating dominant phenotypes. *Development* **118,** 401–415.

Brodsky, M. H., and Steller, H. (1996). Positional information along the dorsal–ventral axis of the *Drosophila* eye: Graded expression of the *four-jointed* gene. *Dev. Biol.* **173,** 428–446.

Bruckner, K., Perez, L., Clausen, H., and Cohen, S. (2000). Glycosyltransferase activity of Fringe modulates Notch-Delta interactions. *Nature* **406,** 411–415.

Cho, K.-O., and Choi, K.-W. (1998). Fringe is essential for mirror symmetry and morphogenesis in the *Drosophila* eye. *Nature* **396,** 272–276.

Dale, L., and Jones, C. M. (1999). BMP signalling in early Xenopus development. *BioEssays* **21,** 751–760.

Golic, K. G., and Lindquist, S. (1989). The FLP recombinase of yeast catalyses site-specific recombination in the *Drosophila* genome. *Cell* **59,** 499–509.

Gubb, D., and García-Bellido, A. (1982). A genetic analysis of the determination of cuticular polarity during development in *Drosophila melanogaster*. *J. Embryol. Exp. Morphol.* **68,** 37–57.

Irvine, K. D. (1999). Fringe, Notch, and making developmental boundaries. *Curr. Opin. Genet. Dev.* **9,** 434–441.

Ito, K., Awano, W., Suzuki, K., Hiromi, Y., and Yamamoto, D. (1997). The *Drosophila* mushroom body is a quadruple structure of clonal units each of which contains a virtually identical set of neurones and glial cells. *Development* **124,** 761–771.

Krasnow, R. E., Wong, L. L., and Adler, P. N. (1995). Dishevelled is a component of the *frizzled* signaling pathway in *Drosophila*. *Development* **121,** 4095–4102.

Lawrence, P. A. (1966). Gradients in the insect segment: The orientation of hairs in the milkweed bug *Oncopeltus fasciatus*. *J. Exp. Biol.* **44,** 607–620.

Lawrence, P. A., Casal, J., and Struhl, G. (1999a). *hedgehog* and *engrailed:* Pattern formation and polarity in the *Drosophila* abdomen. *Development* **126,** 2431–2439.

Lawrence, P. A., Casal, J., and Struhl, G. (1999b). The *hedgehog* morphogen and gradients of cell affinity in the abdomen of *Drosophila*. *Development* **126,** 2441–2449.

Lawrence, P. A., Crick, F. H. C., and Munro, M. (1972). A gradient of positional information in an insect, *Rhodnius*. *J. Cell Sci.* **11,** 815–853.

Lemaire, P., and Yasuo, H. (1998). Developmental signalling: A careful balancing act. *Curr. Biol.* **8,** R228–231.

Panin, V. M., Papayannopoulos, V., Wilson, R., and Irvine, K. D. (1997). Fringe modulates Notch-ligand interactions. *Nature* **387,** 908–912.

Papayannopoulos, V., Tomlinson, A., Panin, V. M., Rauskolb, C., and Irvine, K. D. (1998). Dorsal–ventral signaling in the *Drosophila* eye. *Science* **281,** 2031–2034.

Park, W. J., Liu, J., and Adler, P. N. (1994). Frizzled gene expression and development of tissue polarity in the *Drosophila* wing. *Dev. Genet.* **15,** 383–389.

Piefo, H. (1955). Über die polare Orientierung der Bälge und Schuppen auf dem Schmetterlingsrumpf. *Biol. Zentralbl.* **74,** 467–474.

Rauskolb, C., and Irvine, K. D. (1999). Notch-mediated segmentation and growth control of the *Drosophila* leg. *Dev. Biol.* **210,** 339–350.

Shulman, J. M., Perrimon, N., and Axelrod, J. D. (1998). Frizzled signaling and the developmental control of cell polarity. *Trends Genet.* **14,** 452–458.

Speicher, S. A., Thomas, U., Hinz, U., and Knust, E. (1994). The Serrate locus of *Drosophila* and its role in morphogenesis of the wing imaginal discs: Control of cell proliferation. *Development* **120,** 535–544.

Struhl, G., Barbash, D. A., and Lawrence, P. A. (1997a). Hedgehog acts by distinct gradient and signal relay mechanisms to organise cell type and cell polarity in the *Drosophila* abdomen. *Development* **124,** 2155–2165.

Struhl, G., Barbash, D. A., and Lawrence, P. A. (1997b). Hedgehog organises the pattern and polarity of epidermal cells in the *Drosophila* abdomen. *Development* **124,** 2143–2154.

Strutt, D. I., Weber, U., and Mlodzik, M. (1997). The role of RhoA in tissue polarity and Frizzled signalling. *Nature* **387,** 292–295.

Taylor, J., Abramova, N., Charlton, J., and Adler, P. N. (1998). Van Gogh: A new *Drosophila* tissue polarity gene. *Genetics* **150,** 199–210.

Tokunaga, C., and Gerhart, J. C. (1976). The effect of growth and joint formation on bristle pattern in *D. melanogaster*. *J. Exp. Zool.* **198,** 79–96.

Usui, T., Shima, Y., Shimada, Y., Hirano, S., Burgess, R. W., Schwarz, T. L., Takeichi, M., and Uemura, T. (1999). Flamingo, a seven-pass transmembrane cadherin, regulates planar cell polarity under the control of Frizzled. *Cell* **98,** 585–595.

Villano, J. L., and Katz, F. N. (1995). *four-jointed* is required for intermediate growth in the proximal–distal axis in *Drosophila*. *Development* **121,** 2767–2777.

Vinson, C. R., and Adler, P. N. (1987). Directional non-cell autonomy and the transmission of polarity information by the *frizzled* gene of *Drosophila*. *Nature* **329,** 549.

Vinson, C. R., Conover, S., and Adler, P. N. (1989). A *Drosophila* tissue polarity locus encodes a protein containing seven potential transmembrane domains. *Nature* **338,** 262.

Wehrli, M., and Tomlinson, A. (1998). Independent regulation of anterior/posterior and equatorial/polar polarity in the *Drosophila* eye: Evidence for the involvement of Wnt signaling in the equatorial/polar axis. *Development* **125,** 1421–1432.

Wolff, T., and Rubin, G. (1998). *strabismus*, a novel gene that regulates tissue polarity and cell fate decisions in *Drosophila*. *Development* **125,** 1149–1159.

Xu, T., and Rubin, G. M. (1993). Analysis of genetic mosaics in developing and adult *Drosophila* tissues. *Development* **117,** 1223–1237.

Yuan, Y. P., Schultz, J., Mlodzik, M., and Bork, P. (1997). Secreted *fringe*-like signaling molecules may be glycosyltransferases. *Cell* **88,** 9–11.

Zeidler, M. P., Perrimon, N., and Strutt, D. I. (1999a). The *four-jointed* gene is required in the *Drosophila* eye for ommatidial polarity specification. *Curr. Biol.* **9,** 1363–1372.

Zeidler, M. P., Perrimon, N., and Strutt, D. I. (1999b). Polarity determination in the *Drosophila* eye: A novel rôle for Unpaired and JAK/STAT signalling. *Genes Dev.* **13,** 1342–1353.

Zheng, L., Zhang, J., and Carthew, R. W. (1995). *frizzled* regulates mirror-symmetric pattern formation in the *Drosophila* eye. *Development* **121,** 3045–3055.

Received for publication June 14, 2000
Revised September 12, 2000
Accepted September 12, 2000
Published online November 15, 2000